Applied Catalysis B: Environmental 87 (2009) 84–91

Contents lists available at ScienceDirect

Applied Catalysis B: Environmental

journal homepage: www.elsevier.com/locate/apcatb

Study of Pt–CeO_2 interaction and the effect in the selective hydrodechlorination of trichloroethylene

N. Barrabés [a,b], K. Föttinger [b], A. Dafinov [a], F. Medina [a,*], G. Rupprechter [b], J. Llorca [c], J.E. Sueiras [a]

[a] Dep. d'Enginyeria Química, Universitat Rovira i Virgili, Campus Sescelades, Tarragona 43007, Spain
[b] Inst. of Materials Chemistry, Vienna University of Technology, Veterinaerplatz 1, Vienna A-1210, Austria
[c] Institut de Tècniques Energètiques, Universitat Politècnica de Catalunya, Diagonal 647, 08028 Barcelona, Spain

ARTICLE INFO

Article history:
Received 28 April 2008
Received in revised form 11 August 2008
Accepted 17 August 2008
Available online 28 August 2008

Keywords:
Dechlorination
Trichloroethylene
Pt/CeO_2
Ethylene

ABSTRACT

The feasibility of a catalytic technology to remediate waste streams of halogenated compounds has been improved in order to increase the selectivity towards valuable compounds. Two series of Pt/CeO_2 catalysts prepared by different synthesis protocol, co-combustion and impregnation, have been tested in hydrodechlorination of trichloroethylene in gas phase at mild reaction conditions (temperature between 100 and 300 °C, and 1 bar of pressure). The catalytic behaviour of Pt–Al_2O_3 catalysts was also studied for comparison. Several techniques (BET, XRD, FTIR, HRTEM, etc.) were performed for catalysts characterization. Using the combustion method, the platinum is introduced into ceria matrix, whereas by the impregnation one, the platinum particles are deposited on the surface. In both cases a strong interaction between the support and the platinum particles is observed. Smaller platinum particles sizes are obtained using the impregnation method when compared with the combustion one. When the main product for Pt–Al_2O_3 catalysts was ethane, the use of CeO_2 as support increased the ethylene selectivity. Platinum catalysts obtained by combustion method showed the highest selectivity to ethylene. These results indicate that both the presence of CeO_2 as support and the interaction between ceria and platinum play an important role in the selectivity to ethylene.

1. Introduction

Chlorinated organic compounds like trichloroethene (TCE) are widely distributed pollutants due to their extensive use for metal degreasing or textile cleaning, for example, leading to soil and groundwater contamination. The conversion of industrial by-products like chlorocarbons into more useful or environmentally benign products is nowadays also of great interest. In this sense, hydrodechlorination of chlorinated organics is an attractive alternative to incineration, from both economic and environmental points of view. Noble metals constitute the main catalytic phase for hydrodechlorination due to their high reactivity for the transformation of chlorinated organic compounds into fully hydrogenated products [1,2]. In contrast, several authors demonstrated the ability of *bimetallic* catalysts, composed of metals from Groups VIII and IV, to selectively convert chlorinated alkanes into more valuable alkenes [3,4]. The best performance of these bimetallic catalysts was observed with Pt–Cu [5,6], Pt–Sn [7] and Pd–Ag [3] combinations. The catalytic performance, however, depends on the molar ratio between noble and non-noble metals. Unlike monometallic catalysts, bimetallic deactivate less with time on stream.

The understanding of the carbon–halogen bond dissociation is a key step toward modifying and increasing the activity and selectivity of a catalyst for this reaction. The cleavage of the C–Cl bond has been extensively studied. Metals such as Pt and Pd have been suggested as excellent catalysts for dechlorination reaction [8]. The hydrogenation of TCE on noble metal catalysts may occur following a mechanism similar to the one proposed by Ordónez et al. [9]. The hydrogenation of double bonds would take place catalytically, while the elimination of HCl would be essentially non-catalytic. The hydrogenation of double bonds is favoured as the number of substituents of the double bonds decreases, especially when the atoms are very electronegative (such as chlorine atoms) because it absorbs electron density from the π bond. Ethylene, formed according to the general mechanism, would be quickly hydrogenated on the surface of a very active hydrogenation catalyst such as Pd [1].

With respect to different supports, alumina-supported Pd catalysts were found to exhibit high activity and stability [10,11]. The influence of operation conditions (temperature, hydrogen

* Corresponding author.
E-mail address: francesc.medina@urv.cat (F. Medina).

0926-3373/$ – see front matter © 2008 Elsevier B.V. All rights reserved.
doi:10.1016/j.apcatb.2008.08.018

flow, pressure, etc.) on both activity and selectivity has also been studied. It was found that higher reaction temperatures lead to higher initial activity but also to faster deactivation, and the high hydrogen flow rates have the same effect [12]. Catalyst deactivation in gas-phase hydrodechlorination has been linked to different phenomena. The poisoning of the active phase by the HCl formed in the reaction was proposed by many authors as the main cause of deactivation [9,10,13]. Other works claimed that this phenomenon is not so important for several noble metals (including Pd) and suggested that metal particle sintering and coke deposition [12,14] were the main causes of deactivation. One point is that HCl can react with inorganic supports, such as alumina, causing an increase of surface acidity (Al chlorides are strong Lewis acids), which may favour the formation of carbonaceous deposits on the catalyst surface [15]. Thus, the development of poison-resistant catalysts has gained significant importance in the recent years. The activity of the noble metal is influenced by several factors like method of preparation and metal particle size [16]. Furthermore, the metal–support interaction also contributes to the change in the nature of the active sites, especially when noble metal is supported on reducible metal oxides such as TiO_2, CeO_2, Nb_2O_5 and La_2O_3 [17,18].

On the other hand, in heterogeneously catalyzed processes, structure effects are the most significant parameters governing the catalytic properties of the metal [16]. Ceria-based oxides are widely used for automotive catalysts because of their performance, not only in storing/releasing oxygen, but also in stabilizing precious metal dispersion. Several studies have dealt with Pt sintering and Pt-support interaction in Pt/ceria catalysts. Using laser Raman, Murrell et al. [19] showed that the precious metal interacts strongly with the ceria surface. Nagai et al. [20] showed how the oxygen electron density in the oxide support influences the strength of the Pt–O–M bond, controlling the sintering of supported Pt particles on CeO_2.

It has been demonstrated that for the crotonaldehyde hydrogenation reaction, the selective hydrogenation of the carbonyl bond occurs when the metal has a strong interaction with the support (CeO_2) [21,22]. However, the origin of the specific catalytic behaviour of platinum in SMSI (strong metal support interaction) state is still a matter of debate: formation of Pt–Ce alloy [23], electronic effect on platinum particles due to the partial reduction of ceria [21,24], decoration of platinum particles by patches of partially reduced ceria, etc. [25].

The purpose of this work is to examine the performance of Pt–Al_2O_3 and Pt–CeO_2 catalysts for the selective hydrodechlorination of trichloroethylene to ethylene. The Pt–CeO_2 catalysts were prepared by different methods in order to understand how the interaction between platinum and ceria affects the catalytic performance.

The nanostructure and properties of the catalysts have been examined by high-resolution transmission electron microscopy (HRTEM), X-ray diffraction (XRD), temperature programmed reduction (TPR), hydrogen chemisorption and Fourier transformed infrared spectroscopy with CO as probe molecule (FTIR-CO).

2. Experimental

2.1. Catalysts synthesis

Two procedures have been followed for Pt–CeO_2 preparation, impregnation (I) and solution co-combustion (C). For the synthesis of CeO_2, a mixture of cerium ammonium nitrate (7.50 g), Pluronic (0.21 g) and 4 ml of ethanol were stirred in a Pyrex dish (500 ml). The homogeneous mixture was then moved to a muffle furnace preheated to 350 °C. The solution boiled with foaming and frothing and ignited to burn with a flame yielding about 2.5 g of voluminous oxide product within ca. 5 min. The ceria support was then impregnated via the incipient-wetness technique, using an ethanol solution of H_2PtCl_6. Thereafter, catalysts were dried at 120 °C for 24 h, calcined at 200 °C for 2 h and reduced at 350 °C in hydrogen flow for 3 h. In the second method (co-combustion method (C)), different amounts of the platinum salt were introduced in the initial mixture containing cerium ammonium nitrate, pluronic and ethanol. The homogeneous mixture, introduced into the muffle furnace preheated to 350 °C, was yielding a voluminous cerium oxide powder containing the platinum.

2.2. Sample characterization

Powder X-ray diffraction patterns of the different samples were obtained with a Siemens D5000 diffractometer using nickel-filtered Cu Kα radiation. The patterns were recorded over a range of 2θ angles from 10° to 90° and crystalline phases were identified using the Joint Committee on Powder Diffraction Standards (JCPDS) files. Temperature programmed reduction (TPR) studies of the samples were performed using a TPD/R/O 1100 (Thermo-Finnigan) equipped with a thermal conductivity detector (TCD) and coupled to a mass spectrometer QMS 422 Omnistar. Before the TPR, the sample (around 100 mg) was dried under flowing helium (20 ml/min) at 120 °C for 24 h. After that, the reduction process was carried out between room temperature and 800 °C at a heating rate of 20 °C/min flowing the reducing gas mixture (5% H_2 in argon with a flow of 20 ml/min).

The Fourier transformed infrared (FT-IR) spectra were recorded on a Bruker IFS 28 instrument with a resolution of 4 cm^{-1}. The spectrometer cell is connected to a vacuum system working in the 10^{-6} mbar range and to a heating system. The cell can be used for in situ pre-treatments of samples and adsorption of gases. The samples were pressed into self-supporting wafers that were placed inside a ring furnace in the vacuum cell. The catalysts were reduced in situ using 500 mbar of pure H_2. The catalysts were heated until 300 °C in hydrogen atmosphere using a temperature ramp of 10 °C/min and kept at that temperature for 30 min. After the reduction, the cell was evacuated for 30 min. The CO adsorption measurements were carried out using 5 mbar of pure CO.

High-resolution transmission electron microscopy (HRTEM) was carried out with a JEOL 2010F instrument equipped with a field emission gun. The point-to-point resolution was 0.19 nm and the resolution between lines was 0.14 nm. Samples were deposited on holey-carbon coated grids from alcohol suspensions. At least one hundred particles were used for particle size distribution calculation.

A hydrogen chemisorption analysis was carried out in a Micromeritics ASAP 2010 apparatus. Samples were previously reduced in the same conditions in which the catalysts were prepared. After reduction, the hydrogen on the metal surface was removed with 30 ml/min of He for 30 min at 683 K. The sample was subsequently cooled to 303 K under the same He stream. The chemisorbed hydrogen was analyzed at 343 K using the adsorption–backsorption isotherm method.

2.3. Catalytic activity

The catalysts were tested in the hydrodechlorination reaction of trichloroethylene (TCE) using a continuous fixed-bed glass reactor in the range of 100–300 °C, at atmospheric pressure and stoichiometric amounts of hydrogen. The gas feed is obtained flowing an inert gas (He) and hydrogen through a saturator (at T = 25 °C) containing Trichloroethylene in liquid phase. The gas flows are adjusted by mass flow controller and introduced into the

Table 1
Reaction conditions

Temperature (°C)	100–300
H_2 flow (ml/min)	14
He flow (ml/min)	36
TCE partial pressure (mbar)	92
Amount of catalyst (mg)	100

reactor, which is placed in an oven coupled with temperature control system. The outside reactor is connected by a six-ways valve to gas chromatograph (using HP-PoraPlot column). For all the experiments, 0.1 g of catalyst was employed. The reaction conditions are shown in Table 1.

3. Results and discussion

3.1. Characterization results

Hydrogen consumption curves (temperature programmed reduction, TPR) of impregnated and combustion Pt/CeO_2 catalysts were measured in the temperature range from 25 to 900 °C, as shown in Fig. 1 and Table 2. H_2-TPR of the CeO_2 support, which is shown for comparison, is characterized by a two broad reduction peaks: the first between 400 and 550 °C and the second reaching temperatures above 700 °C. It is generally accepted that the CeO_2 reduction occurs via a stepwise mechanism, starting with the

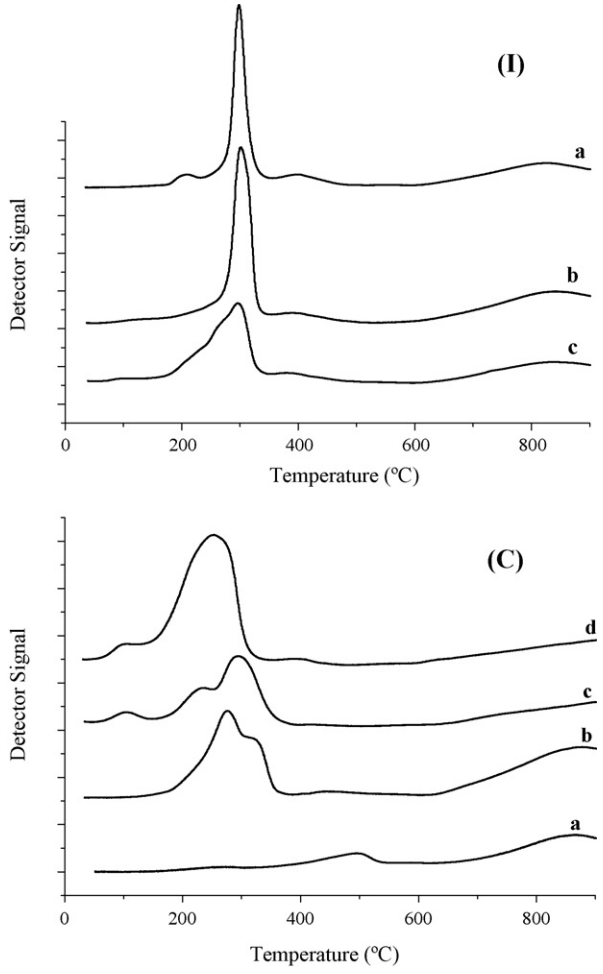

Fig. 1. TPR profiles of Pt/CeO_2 catalysts prepared by impregnation: (I): (a) 0.2%Pt, (b) 0.5%Pt and (c) 1%Pt, and by combustion (C): (a) 0%Pt; (b) 0.2%Pt; (c) 0.5%Pt and (d) 1%Pt.

Table 2
Pt metal dispersion and reduction degree of surface CeO_2 on Pt–ceria catalysts

Catalyst	Calcination temperature (°C)	Metal dispersion[a] (%)	TPR reduction degree of CeO_2 (%)
CeO_2	300	–	4
$0.2Pt/CeO_2$ (I)	300	110	14
	500	53	5
	700	38	4
	900	20	2
$0.5Pt/CeO_2$ (I)	300	75	18.5
$1Pt/CeO_2$ (I)	300	70	15.5
$0.2Pt/CeO_2$ (C)	300	10	14
$0.5Pt/CeO_2$ (C)	300	25	11
$1Pt/CeO_2$ (C)	300	50	24.5

[a] Obtained by H_2 chemisorption.

reduction of the outermost layer of Ce^{4+} (surface reduction) occurring at lower temperature (400–550 °C) whereas the reduction of the inner Ce^{4+} layers (bulk reduction) occurs at higher temperatures (above 700 °C) [26]. The surface shell reduction may involve several phenomena, like: (1) liberation of surface carbonates, (2) reduction of Ce^{4+} surface to Ce^{3+}, and (3) formation of bridging OH groups [21]. The TPR results for the CeO_2 support is in agreement with the results obtained for the reduction of CeO_2 of high surface area [20]. The hydrogen consumption for the first peak represents that around a 4% of the Ce^{4+} surface is reduced to Ce^{3+}. The addition of metals onto the CeO_2 facilitates the surface shell reduction step, likely by reduction of Pt and spillover of hydrogen from the metal to the surface of the oxide, resulting in direct formation of bridging OH groups [22]. This behaviour is indeed observed in Fig. 1(I) for TPR profiles of catalyst with different loadings of Pt incorporated by impregnation. Different peaks between 200 and 450 °C, being related to the reduction of both platinum and CeO_2, were observed. For the 0.2% Pt/CeO_2 (I) sample, the small peak around 200 °C may be attributed to reduction of platinum and ceria in the vicinity of Pt crystallites, as has been suggested by Panagiotopoulou [27]. The main peak detected around 300 °C is mainly due to the reduction of the Ce^{4+} on the surface of the CeO_2 to Ce^{3+} promoted by the addition of platinum. Around a 14% of CeO_2 is reduced to Ce^{3+}. Furthermore, a small peak between 400 and 450 °C that could be related to the reduction of surface ceria that represents 1% is also observed. Similar results are obtained when the platinum content in the sample increases. 18.5% of the surface ceria is reduced at around 300 °C for the 0.5% Pt/CeO_2 (I) sample, while a 15.5% is observed for the 1% Pt/CeO_2 (I) sample.

For the samples prepared by combustion (Fig. 1(C)) broader peaks were observed between 200 and 400 °C and were assigned to the combined reduction of Pt surface species, part of Pt introduced into the ceria lattice and Ce surface species. The broader peaks observed for these samples, in comparison to the impregnation ones, are probably due to diffusion problems of the hydrogen into the $Pt–CeO_2$ system. Because the combustion involves rapid heating, large amounts of gases are generated during the process, leading to crystallite formation. The oxide formed at high temperature is quenched in this process. So in the combustion-derived Pt/CeO_2, Pt ions could either get separated into Pt metal or platinum oxide particles on the oxide support, or platinum ions could get incorporated into the CeO_2 matrix. This behaviour was observed for 0.5% and 1% Pt/CeO_2 (C) samples, which exhibit small TPR peaks at 100 °C attributed to the reduction of Pt^+ to metallic platinum. This peak is not observed for the 0.2% Pt/CeO_2 (C) sample, probably due to the low amount of platinum in the sample. The main reduction peak for these combustion samples is observed between 180 and 350 °C and can be attributed to the reduction

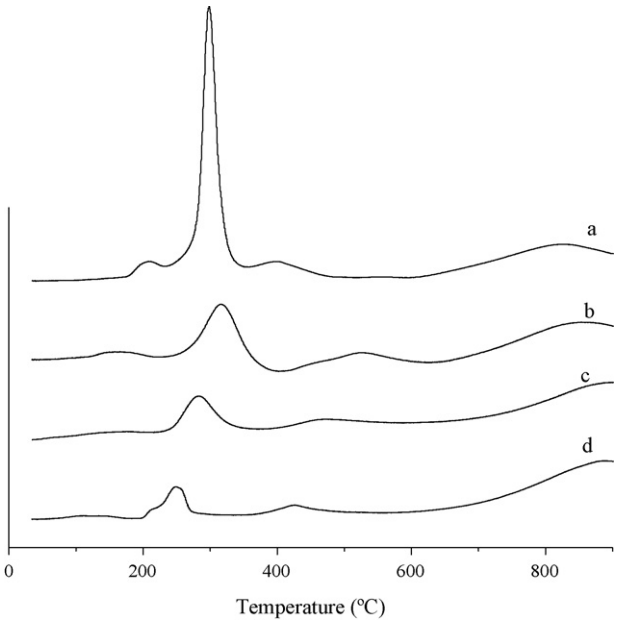

Fig. 2. TPR profiles of 0.2%Pt/CeO_2 (I) calcined at several temperatures: (a) 300 °C; (b) 500 °C; (c) 700 °C; (d) 900 °C.

of the Pt–ceria and the ceria surface. The amount of surface ceria reduced to Ce^{3+} in this range of reduction temperature were 24.5%, 11% and 14.4% for 1%Pt/CeO_2 (C), 0.5%Pt/CeO_2 (C), and 0.2%Pt/CeO_2 (C) samples, respectively (see Table 2).

In order to study the interaction Pt–ceria and the effect of the particle size, the 0.2%Pt/CeO_2 (I) sample was calcined at different temperatures between 300 and 900 °C (see Fig. 2). By increasing the calcination temperature a decrease of the signals of the reduction peaks and a shift to lower reduction temperatures were observed. The amount of CeO_2 reduced was 14, 5, 4 and 2% for the 0.2%Pt/CeO_2 (I) samples calcined at 300, 500, 700 and 900 °C, respectively (see Table 2). The sintering of the platinum particles as well as the support at higher calcination temperatures could explain this behaviour [28].

XRD results show that CeO_2 obtained by combustion method as the samples of Pt/CeO_2 by both methods (C and I) have the typical fluorite-type oxide structure. No phases of Pt were detected. This could be explained by the low amount of noble metal in the samples and the high dispersion.

The platinum dispersion of the samples, obtained by hydrogen chemisorption, is shown in Table 2. The samples obtained by impregnation always showed the highest values of platinum dispersion. When the amount of platinum increased, a slight decrease of the dispersion was observed. The dispersion of the 0.2%Pt/CeO_2 (I) sample was 110% whereas for the 1%Pt/CeO_2 (I) sample was 70%. By increasing the calcination temperature, a decrease in the metal dispersion was observed. The metal dispersion for the 0.2%Pt/CeO_2 (I) sample calcined at 300 °C was of 110% whereas for this sample calcined at 900 °C, a metal dispersion of 20% was detected. Furthermore, the samples obtained by combustion method showed lower metal dispersion values than the obtained by the impregnation method. 10% of metal dispersion was observed for the 0.2%Pt/CeO_2 (C) sample calcined at 300 °C. When the amount of platinum increased the metal dispersion of the combustion samples also increased. The highest metal dispersion for the combustion samples was observed for the 0.2%Pt/CeO_2 (C) sample (around 50%). This fact could be explained by the higher metal particles observed in these samples compared with the impregnated ones. Furthermore, the preparation method, in which some part of the platinum particles could be encapsulated in the ceria matrix, could explain this behaviour.

The samples were analyzed by HRTEM. Fig. 3(I) shows a general view for the sample of 0.5%Pt/CeO_2 (C) after reduction process at low magnification. The sample is comprised by very well dispersed Pt nanoparticles over the CeO_2 support. The size of metal particles is very homogeneous and centred at 3.2 nm. The high dispersion of Pt nanoparticles in the sample merits to be highlighted since more than 90% of all nanoparticles exhibit diameters comprised between

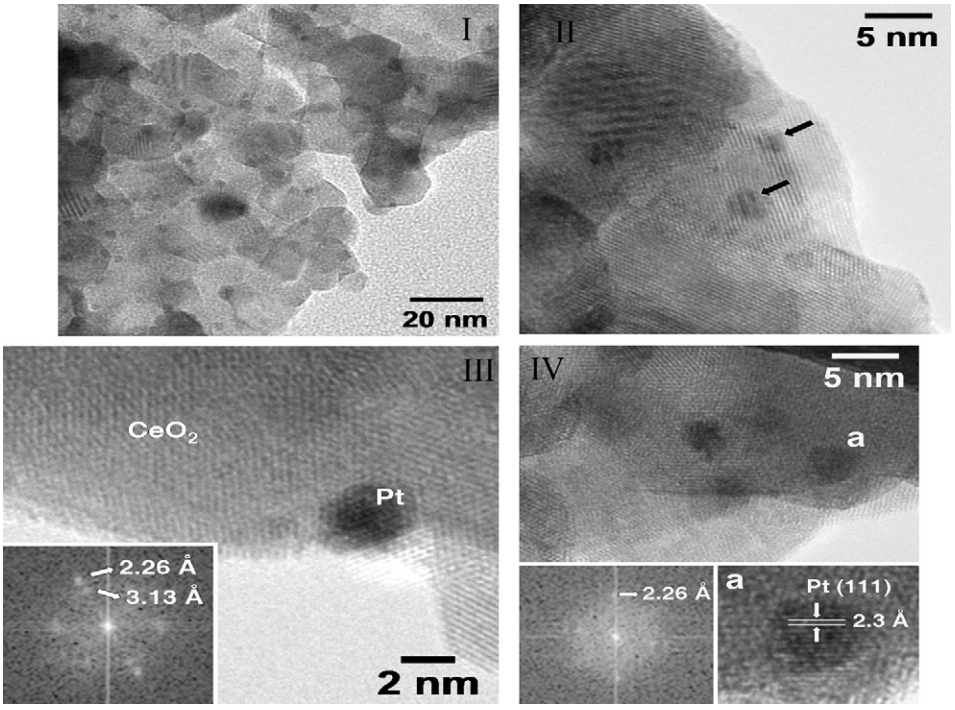

Fig. 3. HRTEM of 0.5Pt/CeO_2 (C) catalyst.

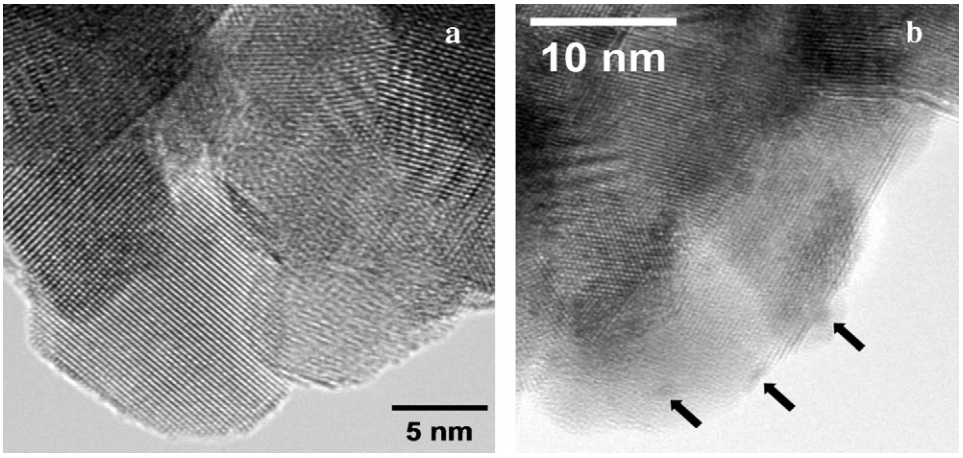

Fig. 4. HRTEM of 0.5%Pt/CeO_2 (I) catalyst.

2 and 4 nm. Two of these Pt nanoparticles are shown at higher magnification in Fig. 3(II) (marked by arrows). Although the particles are not structurally resolved, they show Moiré patterns due to interference with the lattice fringes of the CeO_2 support. Fig. 3(III) shows a detailed image with atomic resolution of the contact area between a Pt nanoparticle and the CeO_2 support. The Fourier transform (FT) image (inset) shows bright spots at 2.26 and 3.13 Å. The spots at 3.13 Å are ascribed to (1 1 1) planes of fcc CeO_2. The occurrence of these spots with less intense spots at 2.7 Å in the FT image at 54.7° indicates that the CeO_2 support crystallite is oriented along the (1 1 0) crystallographic direction. Spots at 2.26 Å correspond to (1 1 1) planes of metallic platinum. The Pt (1 1 1) and CeO_2 (1 1 1) spots are aligned along the same crystallographic direction, strongly suggesting the existence of an epitaxial relationship between them. The sample has been studied in detail over various locations and a large amount of particles exhibited epitaxial relationship with the support, in samples prepared by the combustion synthesis method. Fig. 3(IV) shows other Pt nanoparticles. Particle labeled "a" exhibits lattice fringes at 2.3 Å (2.26 Å in the corresponding FT image), again corresponding to (1 1 1) planes of metallic Pt.

Particles in the sample prepared by impregnation (0.5%Pt/CeO_2 after reduction) are difficult to visualize by transmission electron microscopy due to their extremely small size. Fig. 4(a) shows a typical HRTEM image for this sample, where Pt particles cannot be identified at all. Fig. 4(b) corresponds to another area of the same sample, where various particles of about 1.5 nm in diameter are marked by arrows. Whereas by combustion method epitaxi effect is observed, it has not been possible to perform a similar study over the sample prepared by impregnation, due to the small particle size.

The mean diameter of nanoparticles, in both samples, was determined by counting more than one hundred particles and it is around 1.7 nm for impregnated ones; although it may be easily lower than that given the difficulties in identifying by TEM particles smaller than 1 nm. No structural information can be obtained by HRTEM on such small particles. Whereas by the combustion method, the sample is centred at 3.2 nm, as it is shown at the histogram in Fig. 5.

The IR spectra obtained after room temperature CO exposure of impregnated (I) and co-combustion (C) Pt/CeO_2 catalysts (after prior H_2 reduction at 350 °C) are shown in Fig. 6. The results show that the CO is not adsorbed on CeO_2 (except for carbonates species; not shown [29]). For Pt containing catalysts, CO not well resolved bands were observed between 2120–2130 cm^{-1} and 2080–2070 cm^{-1}. P. Panaglotopoulou et al. [27] proposed that Ce cations influence the adsorption state of CO by enhancing the back-bonding through the metal. The strong bands observed at around 2068 and 2083 cm^{-1} are attributed to CO linearly bonded to surface-exposed metal Pt atoms [30]. The Pt–CO IR band at 2083 $cm^{-1}$is indicative of the presence of metal atoms in less dense close packing arrangements such as 100 faces, while the CO low-frequency band at 2068 cm^{-1} is related to the presence of Pt atoms in defect sites (steps and corners) [24,30–32]. These results are in agreement with the observations made previously by TEM. Interestingly, no IR bands of Pt-dicarbonyl species (1984 cm^{-1}) and bridge CO species (1908 cm^{-1}) were detected [33]. This fact could be explained by a high dispersion of the Pt in the CeO_2 matrix.

The bands assignment in the region 2130–2110 cm^{-1} is a matter of controversy; the general assignment for the Pt–CeO_2 system is shown in Table 3. The bands between 2120 and 2130 cm^{-1} may have different origins, but it is mainly attributed to the presence of oxidized Pt in Pt/CeO_2. Pt is shown to be bonded to surface lattice oxygen and this kind of bond is not fully reducible even at high reduction temperature. Since the vibrational frequency of adsorbed CO is higher when the state of metal is more positive, the bands between 2120 and 2130 cm^{-1} may be due to CO

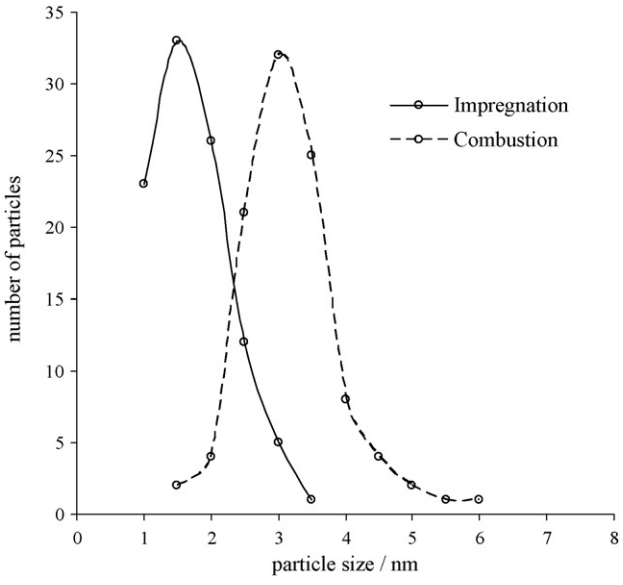

Fig. 5. Histogram of particle size of 0.5%Pt/CeO_2 catalyst.

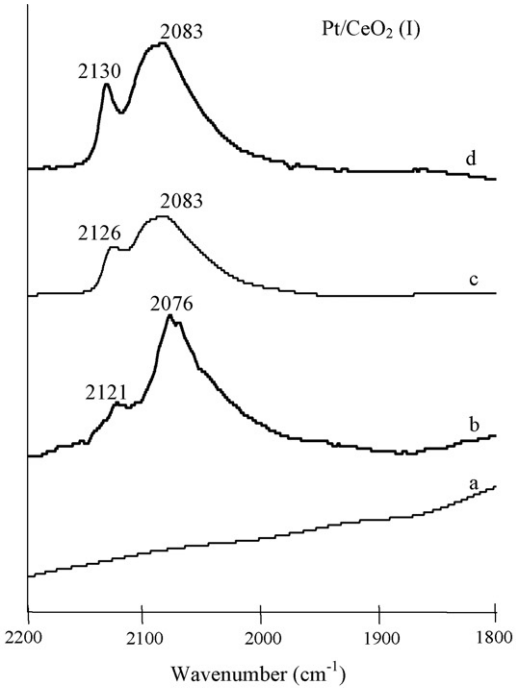

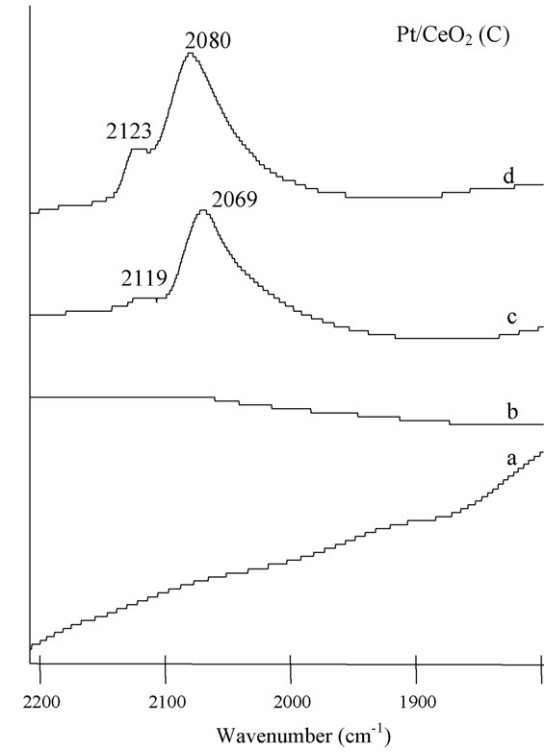

Fig. 6. FTIR profiles of Pt/CeO_2 impregnated (I) and combustion (C) catalysts. Profile of CO adsorption followed by short evacuation at room temperature. (a: ceria; b:0.2%Pt; c:0.5%Pt; d:1%Pt).

linearly adsorbed on Pt atoms interacting with oxygen; i.e., Pt atoms are in a more unsaturated coordination state ($Pt^{\delta+}$), probably created by a strong metal–support interaction (SMSI) [30]. On the other hand, these bands may also be attributed to the adsorption of CO on Ce^{3+}, as well as to the presence of species like Cl. The presence of Ce^{3+} on the surface is related to a reduction of the CeO_2 promoted by the noble metal as has been detected by TPR. The presence of Cl species could arise from the precursor salt of

Table 3
IR bands assignment on ceria and Pt/Ceria

Wavenumber (cm^{-1})	Surface species[a]
2085–2068	CO linearly adsorbed on reduced Pt^0 platinum sites. OC–Pt^0 without Ce^{3+} interaction
2030–2062	OC–Pt^0 with Ce^{3+} interaction
2120–2127	CO linearly adsorbed on Ce^{3+} or on partially oxidized Pt
1820–1840	Bridge-bonded CO on Pt^0 sites
1765	Pt^0–CO–Ce^{3+}
1700–1690	Pt_2^0–CO–Ce^{2+}
1641–1045	Surface formate and/or carbonate species (associated support)

[a] Refs. [19,20,22,24,25].

platinum (H_2PtCl_6) [34]. In addition, using XRD Bera et al. [35] reported the formation of $Ce_{1-x}Pt_xO_{2-\delta}$ and the absence of platinum oxide phases in Pt/CeO_2 prepared by combustion. However, due to the low amount of Pt in the sample, surface PtO_x phase is difficult to detect by XRD. As a conclusion the IR results indicates a strong interaction between platinum and the support for the Pt–CeO_2 samples. However, for the 0.2%Pt/CeO_2 (C) catalyst, no CO adsorption was observed, probably due to the encapsulation of Pt in the CeO_2 matrix.

Furthermore, when the calcination temperature was increased for the 0.2%Pt/CeO_2 (I) sample, some changes in the IR spectra were

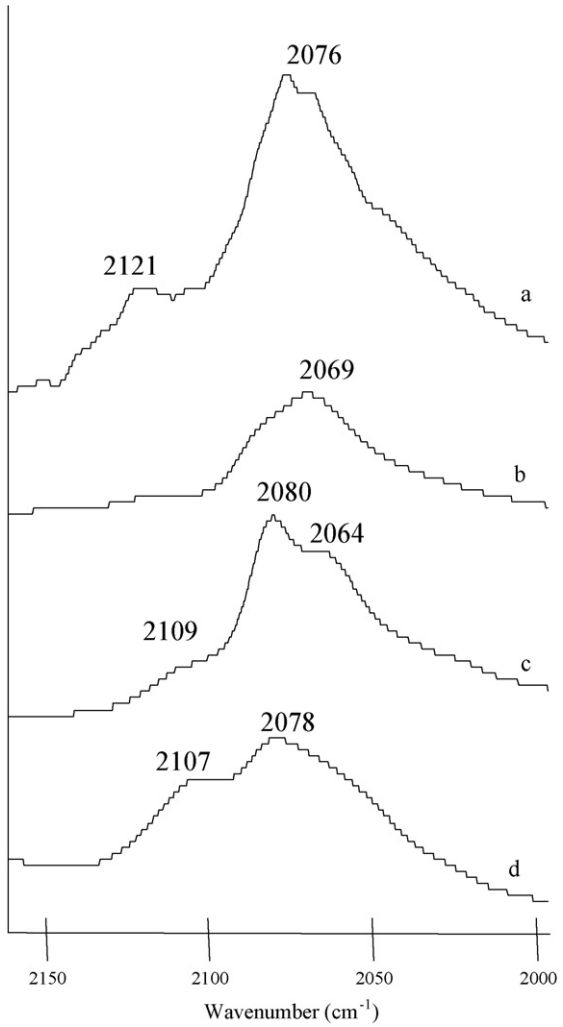

Fig. 7. CO-FTIR of 0.2%Pt/CeO_2 (I) catalyst calcined at several temperatures: (a) 300 °C; (b) 500 °C; (c) 700 °C; (d) 900 °C.

observed (see Fig. 7). Increasing the calcination temperature from 300 to 500 °C, and after reduction, the IR band located at 2121 cm^{-1} disappears. This could be explained considering that at this calcination temperature the chloride species are removed from the surface as has been detected by EDS analysis. When the calcination temperature increased up to 700 and 900 °C, a new band at around 2110 cm^{-1} was detected. The intensity of this band increases with the increase of the calcination temperature. These facts indicate different CO–Pt interactions by modification of the calcination temperature.

3.2. Catalytic activity results

The catalytic behaviour of Pt/CeO_2 catalysts, in the hydrodechlorination reaction of TCE, obtained by combustion (C) and impregnation methods (I), at a reaction temperature of 300 °C and a molar ratio between TCE/H_2 = 1/3, is shown in Fig. 8 (the reaction conditions are listed in Table 1). In all cases the conversion increases for higher platinum loadings. However, the selectivity to ethylene decreased. The catalysts obtained via combustion and by impregnation show similar activities. But the selectivity towards ethylene is higher for the combustion derived catalysts. To study the effect of the support in the selectivity to ethylene, a $1\%Pt/Al_2O_3$ catalyst was tested at the same reaction conditions. Changing the WHSV, conversions of TCE from 10% up to 100% were obtained. However, in all cases the selectivity to ethane was 100%. Consequently the product obtained using the $1\%Pt/Al_2O_3$ catalyst is always the full hydrogenated compound. The difference between $Pt–CeO_2$ and $Pt–Al_2O_3$ catalysts could be attributed to a different metal–support interaction that has been observed by different characterization techniques. Considering that the highest selectivity to ethylene was obtained for the $0.2\%Pt–CeO_2$ catalysts, a study of the influence of the reaction temperature was performed. Fig. 9 shows the catalytic behaviour of the 0.2% $Pt–CeO_2$ catalysts obtained by combustion (C) and by impregnation (I) in the TCE hydrodechlorination reaction. As expected, the conversion increased when the reaction temperature increased from 100 up to 300 °C. A TCE conversion of around 3% was obtained for combustion and impregnation catalysts when the reaction temperature was 100 °C. When the reaction temperature was of 300 °C the TCE conversion increased at around 12%, for both catalysts. A slight increase in the selectivity to ethylene was obtained for the combustion catalysts with respect to the impregnation ones, when the reaction temperature was between 100 and 200 °C. The highest difference in the selectivity to ethylene was obtained working at higher reaction temperature (300 °C). Selectivity to ethylene of around 50% was obtained for

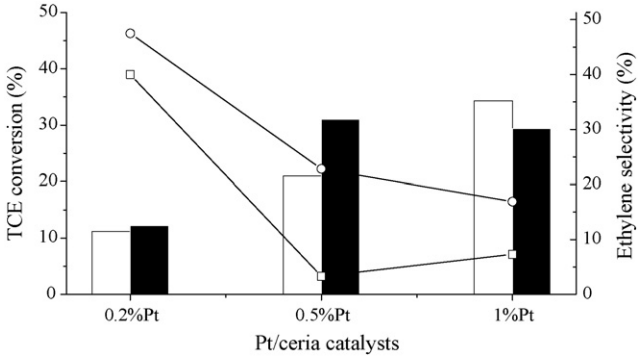

Fig. 8. Catalytic results in the hydrodechlorination reaction of trichloroethylene at T = 300 °C at H_2/TCE stoichiometric molar ratio and 0.1 g of catalyst (□: TCE conversion with (C); ■: TCE conversion with (I); -□-: ethylene selectivity with (I); -○- ethylene selectivity with (C)).

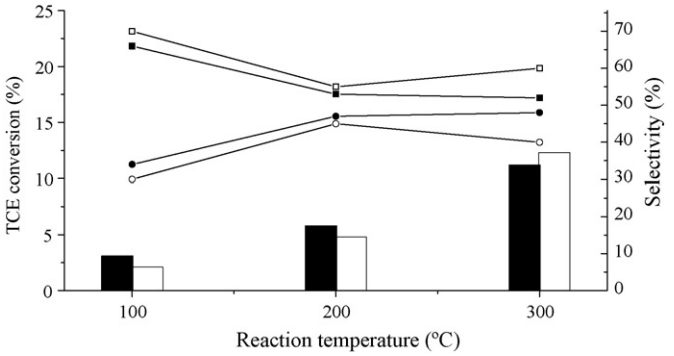

Fig. 9. Catalytic results in the hydrodechlorination reaction of trichloroethylene with $0.2\%Pt/CeO_2$ by combustion (C) and impregnation (I) methods (□:: TCE conversion with (I); ■: TCE conversion with (C); -□-: ethane selectivity; -○- ethylene selectivity).

the $0.2\%Pt–CeO_2$ (C) catalyst, whereas a 40% of selectivity to ethylene was obtained for the $0.2\%Pt–CeO_2$ (I). Interestingly, the fact of increasing the reaction temperature produces an increase in the conversion as well as in the selectivity to ethylene. This could be explained because at higher reaction temperature, the diffusion rate increases and the adsorption strength decreases, both leading to shorter residence time of TCE on the active sites of the catalysts.

On the other hand, when the calcination temperature of the $0.2\%Pt–CeO_2$ (I) catalyst increased from 300 up to 900 °C, an increase in the TCE conversion was observed (see Table 4). However, a decrease in the selectivity of ethylene was also observed. This fact could indicate that the high calcination temperatures can produce a segregation of the Pt particles diminishing the interaction between Pt and CeO_2 as has been observed by TPR. Besides, the metal dispersion of the platinum decreased from 110% to 20% when the calcination temperature increased from 300 up to 900 °C. Consequently, the free metal platinum particles have a strong activity for hydrodechlorination but a low selectivity to the olefin obtaining (mainly) the full hydrogenated product in similar way that the results obtained for the $Pt–Al_2O_3$ catalyst.

Furthermore, the stability of some catalysts has been studied for a reaction time of around 24 h as it is shown in Fig. 10. After a slight conversion decrease during the first hour of reaction the activity of the catalysts remained practically constant. Besides, the selectivity to ethylene remained constant.

From our results, the selectivity to ethylene using $Pt–CeO_2$ catalysts in the hydrodechlorination reaction of TCE is influenced by several parameters. Small platinum particles sizes (lower than 2 nm), that are obtained using the impregnation method, show a higher selectivity to full hydrogenated compounds (ethane). This could be explained considering that small metallic particles are often described as electron deficient species, less reactive towards electrophilic adsorbates like Cl, but presenting enhanced reactivity towards nucleophilic compounds [13]. Small particles, with low electron density of d-orbital, present higher selectivity to deep-

Table 4
Catalytic activity of $0.2\%Pt/CeO_2$ (I) (T = 300 °C; H_2/TCE stoichiometric. molar ratio; 0.1 g catalyst)

T calcinations (°C)	Conversion TCE (%)	Selectivity ethane (%)	Selectivity ethylene (%)
300	12	60	40
500	37	73	27
900	69	84	11
900[a]	15	83	15

[a] The flow rate of reagents have been increased in 5 times.

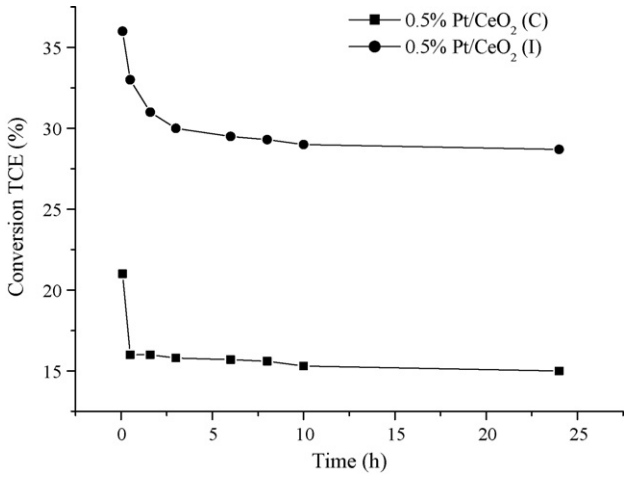

Fig. 10. Study of catalyst deactivation during the hydrodechlorination reaction of trichloroethylene at $T = 300$ °C at H_2/TCE stoichiometric molar ratio and 0.1 g of catalyst.

dechlorinated compounds due to the strong adsorption strength of chlorinated compounds and the large amount of activated hydrogen [28]. Besides, the coverage by Cl is higher at high conversion and on larger metal particles (small particles are chlorinated at a lower rate) [13]. These facts could explain the higher selectivity to ethylene observed using the combustion method where larger platinum particles between 2 and 4 nm are obtained.

On the other hand, it is well known that the modification of supported platinum catalysts by the addition of a second metal changes dramatically the catalytic performance for chlorocarbon dechlorination; the catalysts become highly selective toward olefins [4]. This has been observed in the hydrodechlorination reaction of 1,2-dichloroethane using Pt–Cu/C catalysts [36]. While Pt catalyzes the hydrodechlorination reaction of vicinal chlorocarbons to form saturated hydrocarbons, the modification of the noble metal with another metal shifts the reaction toward hydrogen assisted dechlorination to form the corresponding olefinic products [4]. From our results, the interaction between platinum and CeO_2 plays a similar role to the addition of a non-noble metal. The presence of Ce^{3+} in the catalysts could interact with chlorine of the TCE obtaining the dechlorination product. Then, assisted by hydrogen, coming from platinum metal, the surface is regenerated. Contrarily, when the TCE is adsorbed on the metal particle (Pt), a deep hydrogenation is performed. Consequently, the metal–support interaction and the metal particle size govern both activity and selectivity in the hydrodechlorination reaction of TCE. However, the mechanism of this phenomenon requires further investigations.

4. Conclusions

This work shows that, by modifying the synthesis protocol (combustion and impregnation), different platinum particle sizes and metal support interactions are obtained. Using the impregnation method smaller platinum particles are obtained when compared with the combustion ones. Furthermore, Pt–CeO_2 catalysts have shown high stability, activity and selectivity in the selective hydrodechlorination reaction of trichloroethylene to obtain ethylene. The catalytic behaviour depends on the used method for catalysts preparation. High interaction between platinum and the support is the key to obtain selective catalysts. However, more studies are certainly required to have a deep understanding about the interaction of platinum and the ceria support.

Acknowledgments

The authors thank Ministerio de Educación y Ciencia, Ministerio de Medio Ambiente and Generalitat de Catalunya (Spain) for financial support, projects: A196/2007/2-07.1; 246/2006/3-7.1; HU2006-0026, 246/2006/3-7.1 and Q9999/2007/309-118, respectively. The authors also thank the Austrian Academic Exchange Service for financial support; project ES 05/2007 (Acciones Integradas).

References

[1] S. Ordónez, F.V. Diez, H. Sastre, Ind. Eng. Chem. Res. 41 (2002) 505–511.
[2] C.G. Schreier, M. Reinhard, Chemosphere 31 (1995) 3475–3487.
[3] S. Lambert, F. Ferauche, A. Brasseur, J.P. Pirard, B. Heinrichs, Catal. Today 100 (2005) 283–289.
[4] V.I. Kovalchuk, J.L. d'Itri, Appl. Catal. A: Gen. 271 (2004) 13–25.
[5] V.Y. Borovkov, D.R. Luebke, V.I. Kovalchuk, J.L. d'Itri, J. Phys. Chem. B 107 (2003) 5568–5574.
[6] V.Y. Borovkov, D.R. Luebke, V.I. Kovalchuk, J.L. d'Itri, Abstr. Pap. Am. Chem. S 225 (2003) U140–U1140.
[7] W.D. Rhodes, K. Lazar, V.I. Kovalchuk, J.L. d'Itri, J. Catal. 211 (2002) 173–182.
[8] L.A.M.M. Barbosa, P. Sautet, J. Catal. 207 (2002) 127–138.
[9] S. Ordónez, H. Sastre, F.V. Diez, Appl. Catal. B: Environ. 25 (2000) 49–58.
[10] S. Ordónez, H. Sastre, F.V. Diez, Appl. Catal. B: Environ. 29 (2001) 263–273.
[11] E. Finocchio, G. Sapienza, M. Baldi, G. Busca, Appl. Catal. B: Environ. 51 (2004) 143–148.
[12] S. Ordónez, H. Sastre, F.V. Diez, Appl. Catal. B: Environ. 40 (2003) 119–130.
[13] B. Coq, G. Ferrat, F. Figueras, J. Catal. 101 (1986) 434–445.
[14] S. Ordónez, E. Diez, H. Sastre, Catal. Lett. 72 (2001) 177–182.
[15] B. Coq, J.M. Cognion, F. Figueras, D. Tournigant, J. Catal. 141 (1993) 21–33.
[16] R. Gopinath, N. Lingaiah, N. Seshu Babu, I. Suryanarayana, P.S. Sai Prasad, A. Obuchi, J. Mol. Catal. A: Chem. 223 (2004) 289–293.
[17] S.T. Srinivas, P.S.S. Prasad, S.S. Madhavendra, P. Kanta Rao, Studies Surf .Sci. Catal. 113 (1998) 835–839.
[18] R. Gopinath, K. Narasimha Rao, P.S. Sai Prasad, S.S. Madhavendra, S. Narayanan, G. Vivekanandan, J. Mol. Catal. A: Chem. 181 (2002) 215–220.
[19] L.L. Murrell, S.J. Tauster, D.R. Anderson, F. Bozonverduraz, S.I. Woo, W.C. Conner, J.C. Conesa, D.G. Blackmond, M. Ichikawa, C.H. Bartholomew, Studies Surf. Sci. Catal. 75 (1993) 681–690.
[20] Y. Nagai, T. Hirabayashi, K. Dohmae, N. Takagi, T. Minami, H. Shinjoh, S. Matsumoto, J. Catal. 242 (2006) 103–109.
[21] G. Jacobs, S. Ricote, B.H. Davis, Appl. Catal. A: Gen. 302 (2006) 14–21.
[22] M. Abid, V. Paul-Boncour, R. Touroude, Appl. Catal. A: Gen. 297 (2006) 48–59.
[23] M. Abid, G. Ehret, R. Touroude, Appl. Catal. A: Gen. 217 (2001) 219–229.
[24] P. Concepcion, A. Corma, J. Silvestre-Albero, V. Franco, J.Y. Chane-Ching, J. Am. Chem. Soc. 126 (2004) 5523–5532.
[25] S. Bernal, J.J. Calvino, M.A. Cauqui, J.M. Gatica, C.L. Cartes, J.A.P. Omil, J.M. Pintado, Catal. Today 77 (2003) 385–406.
[26] H.C. Yao, Y.F.Y. Yao, J. Catal. 86 (1984) 254–265.
[27] P. Panagiotopoulou, J. Papavasiliou, G. Avgouropoulos, T. Ioannides, D.I. Kondarides, Chem. Eng. J. 134 (2007) 16–22.
[28] J.W. Bae, J.S. Lee, K.H. Lee, Appl. Catal. A: Gen. 334 (2008) 156–167.
[29] K. Föttinger, R. Schlögl, G. Rupprechter, Chem. Commun. (2008) 320–322.
[30] B.A. Riguetto, S. Damyanova, G. Gouliev, C.M.P. Marques, L. Petrov, J.M.C. Bueno, J. Phys. Chem. B 108 (2004) 5349–5358.
[31] C.B. Binet, A.J.C. Lavalley, J. Phys. Chem. 98 (1994) 6392.
[32] A.M. Bensalem, J.C. Tessier, D. Bozon-Verduraz, J. Chem. Soc. Faraday Trans. 92 (1996) 3233.
[33] A.C. Concepción, P.J. Silvestre-Albero, Top. Catal. 46 (2007) 31–38.
[34] L. Kepinski, J. Okal. 192 (2000) 53.
[35] P. Bera, K.R. Priolkar, A. Gayen, P.R. Sarode, M.S. Hegde, S. Emura, R. Kumashiro, V. Jayaram, G.N. Subbanna, Chem. Mater. 15 (2003) 2049–2060.
[36] D.R. Luebke, L.S. Vadlamannati, V.I. Kovalchuk, J.L. d'Itri, 35 (2002) 217.